Geophysical Journal International

Geophys. J. Int. (2015) **202,** 454–463 doi: 10.1093/gji/ggv162
GJI Marine geosciences and applied geophysics

Crustal structure of the Murray Ridge, northwest Indian Ocean, from wide-angle seismic data

T.A. Minshull,[1] R.A. Edwards[2] and E.R. Flueh[3]

[1]*Ocean and Earth Science, National Oceanography Centre Southampton, University of Southampton, European Way, Southampton SO*14 3*ZH, United Kingdom. E-mail: tmin@noc.soton.ac.uk*
[2]*National Oceanography Centre, European Way, Southampton SO*14 3*ZH, United Kingdom*
[3]*Geomar Helmholtz Centre for Ocean Research, Wischhofstrasse* 1-3, *D-*24148 *Kiel, Germany*

Accepted 2015 April 14. Received 2015 April 13; in original form 2014 October 24

SUMMARY

The Murray Ridge/Dalrymple Trough system forms the boundary between the Indian and Arabian plates in the northern Arabian Sea. Geodetic constraints from the surrounding continents suggest that this plate boundary is undergoing oblique extension at a rate of a few millimetres per year. We present wide-angle seismic data that constrains the composition of the Ridge and of adjacent lithosphere beneath the Indus Fan. We infer that Murray Ridge, like the adjacent Dalrymple Trough, is underlain by continental crust, while a thin crustal section beneath the Indus Fan represents thinned continental crust or exhumed serpentinized mantle that forms part of a magma-poor rifted margin. Changes in crustal structure across the Murray Ridge and Dalrymple Trough can explain short-wavelength gravity anomalies, but a long-wavelength anomaly must be attributed to deeper density contrasts that may result from a large age contrast across the plate boundary. The origin of this fragment of continental crust remains enigmatic, but the presence of basement fabrics to the south that are roughly parallel to Murray Ridge suggests that it separated from the India/Seychelles/Madagascar block by extension during early breakup of Gondwana.

Key words: Controlled source seismology; Continental margins: transform; Indian Ocean.

INTRODUCTION AND GEOLOGICAL SETTING

The northwest Indian Ocean remains one of the least well-understood areas of oceanic lithosphere because a lack of well-mapped magnetic anomaly lineations means that its tectonic history is difficult to unravel, and there are few age constraints for the oceanic lithosphere and overlying sediment. A prominent series of bathymetric highs, including the Murray Ridge, marks the India–Arabia Plate boundary in this region (Fig. 1). Global and local plate circuits (Gordon & Demets 1989; Demets *et al.* 1990) and earthquake focal mechanisms (Quittmeyer & Kafka 1984) suggest a mixture of right-lateral strike slip and oblique extension along this plate boundary. Swath bathymetric mapping of the plate boundary along the Owen Fracture Zone (Fournier *et al.* 2008; Fournier *et al.* 2011) has provided direct evidence of dextral strike-slip motion, and combined with an analysis of relocated earthquakes has allowed the pole of rotation to be more precisely constrained than was previously possible. These authors thereby determined long-term rates of relative motion more tightly to 2–4 mm yr^{-1}. Recent analysis of geodetic data suggests that the present rate of relative motion increases southward from 3.1 ± 0.7 to 3.7 ± 0.7 mm yr^{-1}, with the direction of motion closer to parallel to the plate boundary to the south (ArRajehi *et al.* 2010). The presently active plate boundary is a pure transform boundary, and 12-km offsets across this transform show that the plate boundary has occupied its current location since 3–6 Ma (Fournier *et al.* 2011).

Dalrymple Trough is a pull-apart basin at the northern termination of the Owen Fracture Zone, and Murray Ridge is a bathymetric high that lies to the east of Dalymple Trough and extends to the northeast into the Makran subduction zone. Extensive normal faulting imaged in seismic reflection profiles provides evidence for recent and ongoing extensional deformation within and to the west of Dalrymple Trough (Edwards *et al.* 2000). Wide-angle seismic evidence suggests that the crust to the west of Dalrymple Trough is oceanic, while the crust beneath the Trough is continental (Edwards *et al.* 2008). The active plate boundary in this region is therefore also an ocean–continent boundary. A strong magnetization contrast at the western edge of Dalrymple Trough (Edwards *et al.* 2000) supports this interpretation. Here we present additional wide-angle seismic data that constrain the nature of the crust beneath the Murray Ridge and the abyssal plain to the east and use these and other observations to provide new insights into the tectonic history of this enigmatic region.

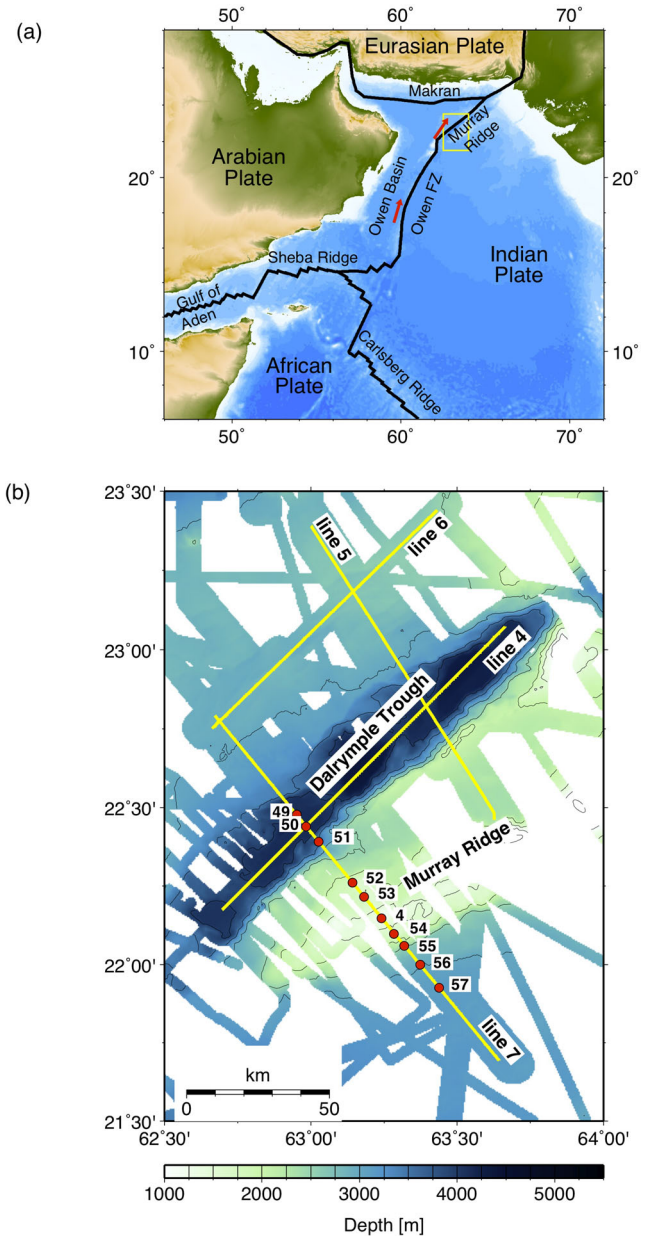

Figure 1. (a) Regional tectonic setting showing plate boundaries. Arrows show the direction of motion of the Arabian Plate relative to the Indian Plate based on the pole of Fournier *et al.* (2011). (b) Bathymetry of Murray Ridge and Dalrymple Trough (area of yellow box in part a). Coloured regions mark areas of swath bathymetric coverage. Yellow lines mark seismic profiles and numbered circles mark ocean bottom hydrophone (49–57) and seismograph (4) positions on line 7.

SEISMIC DATA

Wide-angle seismic data were acquired aboard 'R/V Sonne' in 1997 in a collaborative project between GEOMAR (Kiel), BGR (Hannover) and the University of Cambridge. A grid of profiles was acquired (Fig. 1), coincident with seismic reflection profiles acquired previously (Edwards *et al.* 2000; Gaedicke *et al.* 2002a,b). Up to 10 ocean bottom hydrophones (OBHs) and ocean bottom seismographs (OBSs) were deployed on each profile and these recorded shots from a 51.2 l (3124 cu. in.), 20-airgun array fired at 140 bar with a nominal shot spacing of 150 m (60 s). Lines 4–6 were presented by Edwards *et al.* (2008). These profiles sampled the crustal structure of Dalrymple Trough and the Oman abyssal plain to the northwest, but did not sample the summit of Murray Ridge. Here we focus on line 7, which traversed both Dalrymple Trough and Murray Ridge and extends 30–40 km onto the abyssal plains either side. On this profile the data quality is generally higher in thickly sedimented regions and lower for instruments placed directly on basement outcrops, where there is strong scattering of arrivals (Fig. 2). First arrivals are rarely observed beyond ~30 km offset. A complex set of seismic phases was observed, which can be attributed to up to five distinct sediment layers and two distinct layers within the crystalline crust. The complexity of the structure and the steep topography pose some challenges for interpretation.

SEISMIC MODELLING

Traveltimes of the observed arrivals were picked and assigned uncertainties of ±20, ±30, ±50 or ±100 ms depending on frequency content and signal-to-noise ratio. A single value was used for each observed phase for a given OBH/OBS, but the same phase was sometimes assigned different uncertainties on different instruments according to the signal-to-noise ratio, with larger uncertainties associated with instruments deployed on the steep topography of Murray Ridge.

Given the evidence for multiple layers with distinct velocity discontinuities between them, traveltime tomographic approaches such as those of Zelt & Barton (1998) or Korenaga *et al.* (2000) were not suitable for this data set. Instead, the traveltime data were modelled using the 2-D ray tracing approach of Zelt & Smith (1992) and a combination of forward modelling and limited traveltime inversion, which was used only in flat-lying regions of the model where the inversion was stable. Care was taken not to overparametrize the model; the final model contains the minimum number of depth and velocity nodes necessary to satisfy most of the observed data within their estimated uncertainties. Depth parameter spacing at the seabed was as little as 1 km to reproduce the rough topography of the ridge, and sediment depth parameters also had to be closely spaced in this region, but elsewhere depth parameter spacing was comparable to the seabed instrument spacing. Velocity nodes were spaced more sparsely with additional nodes introduced only where the data required them. The uppermost layers were modelled first, and once a satisfactory traveltime fit (χ^2 approaching 1.0) had been achieved, deeper layers were progressively modelled. At the northwestern end of the profile, where there are limited constraints on the deep structure from the data for this profile, the structure was constrained by crossing Lines 4 and 6 (Edwards *et al.* 2008), which are along-strike of regional structures and therefore show little horizontal variation in velocity.

Because the model is highly heterogeneous, parameter uncertainties will vary greatly between different parts of the model. An attempt was made to estimate model parameter uncertainties using the perturbation approach of Zelt & Smith (1992) in which parameters are varied until rms misfits are no longer acceptable. However, this approach revealed strong trade-offs between the misfit and the number of picks for which rays are successfully traced. Models were rejected if they achieved a lower misfit at the expense of matching fewer picks. These limited tests suggested that the number of picks matched dropped rapidly if layer boundaries were perturbed more than 200 m and if layer velocities were perturbed by more than 0.1 km s^{-1}. True uncertainties are probably at least double these numbers because of trade-offs between velocity and depth and between different parts of the model.

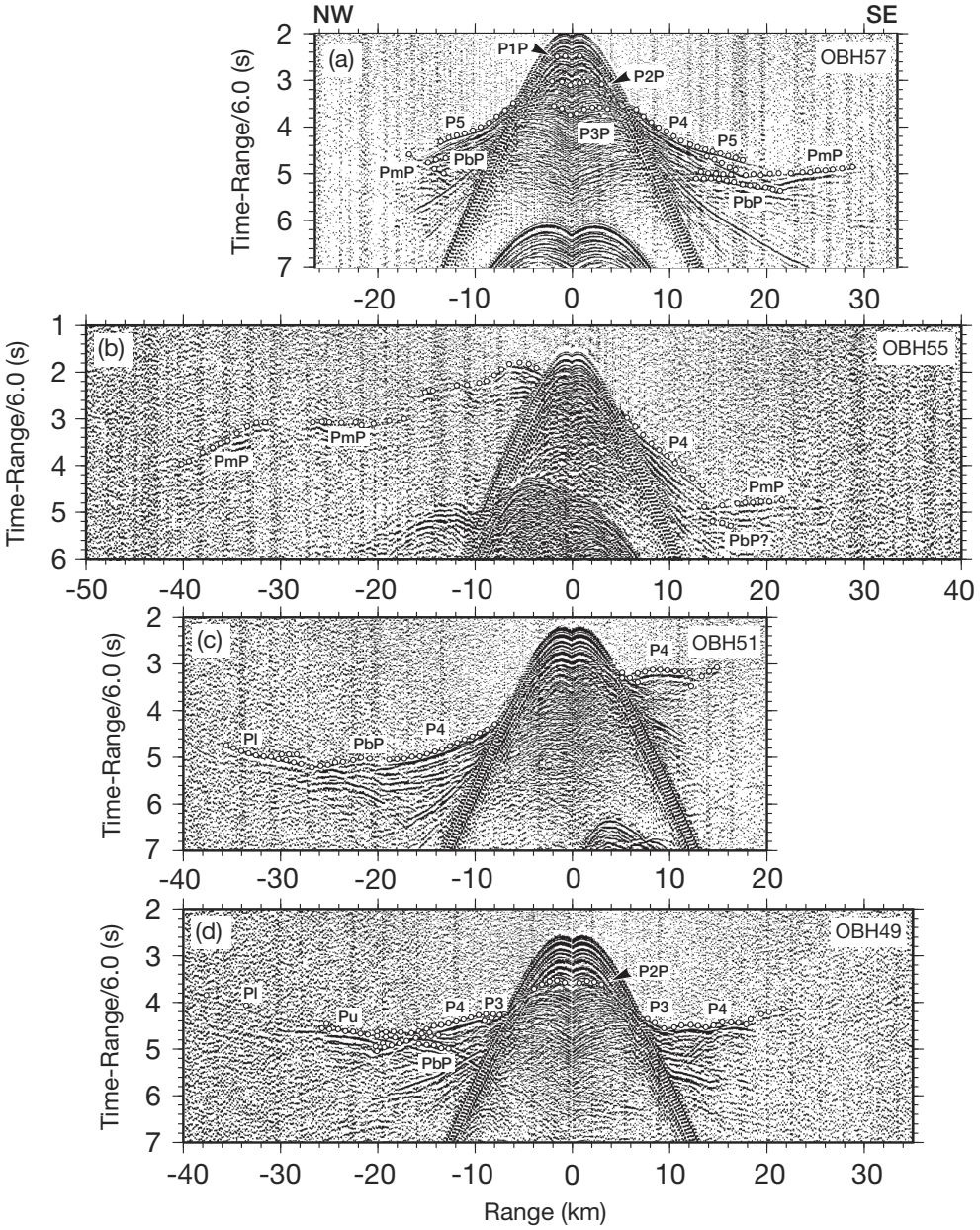

Figure 2. Record section examples. Data are reduced at 6 km s^{-1} and filtered with a zero phase trapezoidal bandpass filter with corner frequencies of 3, 5, 23 and 43 Hz. White circles mark every 5th traveltime pick. Modelled phases are labelled: P1P, P2P and P3P are respectively reflections from the bottom of the 1st, 2nd and 3rd sediment layer; P3, P4 and P5 are, respectively, refractions from the 3rd, 4th and 5th sediment layer; PbP is the reflection from the basement; Pu and Pl are, respectively, refractions from the upper lower crustal layers; and PmP is the Moho reflection. (a) OBH 57 above the Indus Fan; (b) OBH 55 on the southeastern flank of Murray Ridge; (c) OBH 51 on the southeastern edge of Dalrymple Trough; (d) OBH 49 in the centre of Dalrymple Trough.

RESULTS AND DISCUSSION

Seismic velocity model

The quality of the fit achieved is summarized in Table 1. In general a good fit was achieved to reflected and refracted arrivals from the sediment column and to the basement reflection, which is readily picked in the thickly sedimented regions of the profile (Fig. 3). Poorer fits, with misfits reaching twice or even three times the uncertainty, were achieved in regions of steep topography. Here the structure is unlikely to be adequately represented by a 2-D model and picked arrivals may have travelled significantly out of the plane of the profile, so a poorer fit is to be expected. Because such outliers influence L2 norms disproportionately, the overall misfit and chi-squared error are therefore relatively large.

Velocities increase monotonically with depth in the sediments from 1.8–1.9 km s^{-1} close to the seabed to ~4.3 km s^{-1} immediately above the basement in the deepest part of Dalrymple Trough and ~4.5 km s^{-1} immediately above basement to the southeast of Murray Ridge (Fig. 4). Velocities in the uppermost two sediment layers are constrained only by reflections. There is little change in sediment velocity structure across Murray Ridge but the much deeper basement to the southeast (*ca*. 10 km, compared to *ca*. 7 km to the northwest) is evidence for a greater age of the lithosphere in this region.

Table 1. Summary of rms misfits and χ^2 errors between observed and modelled traveltimes for line 7. Phases are identified in Fig. 2, except for sediment reflections from the top three sediments layers denoted as P1P, P2P and P3P. The basement reflection PbP is modelled as a different phase at the southeast (SE) and northwest (NW) ends of the line because an additional sediment layer is present to the southeast.

Phase	Number of picks	Rms misfit (ms)	χ^2 error	Description
P1P	18	15	0.604	Sediment layer 1 reflection
P2P	121	22	1.244	Sediment layer 2 reflection
P3	133	39	2.043	Sediment layer 3 refraction
P3P	38	24	0.657	Sediment layer 3 reflection
P4	424	113	3.622	Sediment layer 4 refraction
PbP (NW)	81	101	4.132	Basement reflection in NW part of model (below layer 4)
PbP (SE)	112	55	0.305	Basement reflection in SE part of model (below layer 5)
P5	106	33	0.451	Sediment layer 5 refraction
All sediment phases	**1033**	**65**	**2.115**	
Pu	445	89	4.144	Refraction from upper crust
PuP	110	43	0.748	Reflection from mid-crustal boundary
Pl	88	63	1.047	Refraction from lower crust
PmP	397	177	3.540	Moho reflection
All crustal phases	**1040**	**126**	**3.292**	
All phases	**2073**	**100**	**2.705**	

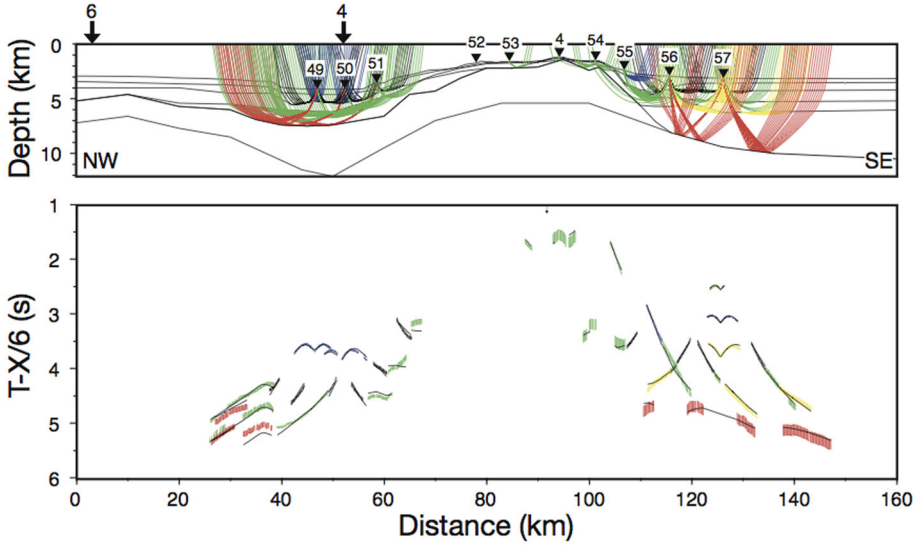

Figure 3. (a) Ray coverage for sediment layers. Rays are plotted for every 3rd traveltime pick. Thin black lines show model boundaries, inverted triangles mark OBH/OBS locations, and arrows mark locations of crossing lines 4 and 6. Black, green and yellow turning rays are from the 3rd, 4th and 5th sediment layer, respectively. Green, blue, yellow and red reflections are from the bottom of the 1st, 2nd, 3rd and 5th sediment layers, respectively. (b) Corresponding traveltime fit. Coloured vertical bars show traveltime picks with their uncertainties, with the same colour coding as in (a); black lines show predicted traveltimes.

Fitting of crustal phases is readily achieved with a simple model towards the ends of the profile, but the steep topography and complex structure of the central part of the profile make it challenging to achieve an adequate fit (Fig. 5). On the northwestern flank of Dalrymple Trough, and consistent with line 6 (Edwards *et al.* 2008), a good fit was achieved using a model with two crustal layers separated by a velocity discontinuity that generates wide-angle reflections. The upper layer has velocities of 4.5–5.4 km s^{-1} and a thickness of 2.5–4.0 km, thickening into the trough, and the lower layer has velocities of 6.4–7.3 km s^{-1} and a thickness of ∼5 km (Fig. 6). Clear Pn arrivals on line 6 (Edwards *et al.* 2008) identify the bottom boundary of the lower layer as the Moho. The thickness of the lower layer and the velocity in the lower part of this layer are poorly constrained by the data presented here, so these parameters are derived primarily from the velocity structure at the crossing with line 6 (Edwards *et al.* 2008). To the southeast of Murray Ridge, constraints come primarily from OBH 57 (Fig. 2a), and the data are well matched by a structure involving a single ∼4 km basement layer with velocities increasing with depth from ∼6.1 to ∼7.4 km s^{-1} (Fig. 6). The base of this layer gives rise to prominent wide-angle reflections indicative of an abrupt velocity discontinuity, so is identified as the Moho despite the absence of identifiable Pn arrivals here.

Beneath the Murray Ridge itself, the crustal structure is complex and laterally variable, and the quality of traveltime fit achieved is poorer (Fig. 5). Velocities at the top of the crystalline crust are constrained by refracted arrivals on several instruments and are in the region of 4.4 km s^{-1}, increasing with depth to ∼5.2 km s^{-1} at 2.5–3.0 km depth into the basement. A strong wide-angle reflection observed on OBS52 (Fig. 5) may come from the base of this layer, indicating an abrupt velocity discontinuity, but no evidence for this discontinuity appears in data from other instruments. Constraints

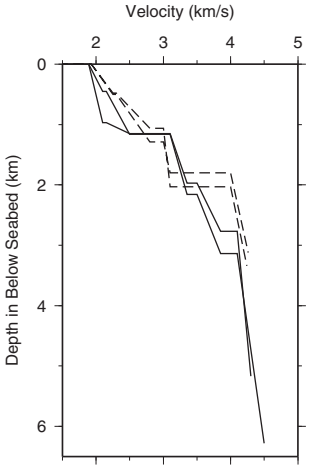

Figure 4. Seismic velocities of sediments. Solid lines mark velocities at model distance 116 and 126 km, on the Indian Plate. Dashed lines mark velocities at model distance 47 and 52 km, in Dalyrymple Trough.

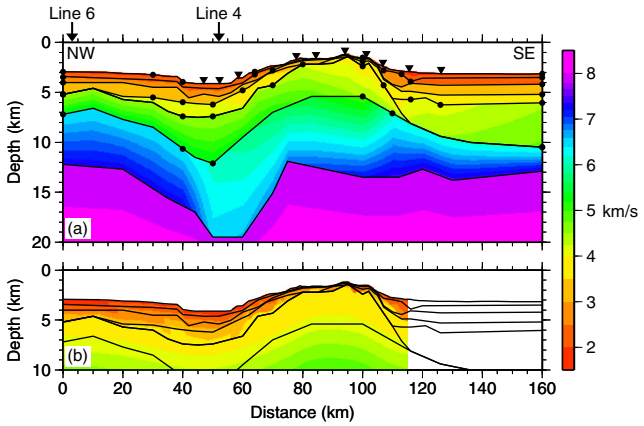

Figure 6. (a) Velocity model from wide-angle seismic data. Inverted triangles mark OBH/OBS locations and arrows mark crossing profiles. Solid lines show model boundaries and filled circles mark velocity nodes in model; for clarity only the nodes at the top of model layers are plotted, but nodes at the bottom of model layers are vertically below these. (b) Velocity model from pre-stack depth migration focusing analysis, overlain by boundaries from (a). In the white region there is no seismic reflection coverage.

on crustal thickness beneath the top of Murray Ridge come from noisy arrivals on OBH55 (Fig. 2b); the predicted traveltimes are too great but moving the Moho to shallower depths degrades the fit for equally noisy arrivals on the adjacent OBH54. The lower crust must be considered as poorly constrained in this region and the poor fit here contributes strongly to a relatively large overall misfit for crustal arrivals (Table 1). However, a good fit to arrivals at OBH51 (Fig. 2c) which traverse Dalrymple Trough, is achieved with velocities of 6.1–6.5 km s^{-1} in this lower layer, consistent with the very low velocities obtained in the lower crust on the crossing line 4 by Edwards *et al.* (2008). The model includes an abrupt contrast between these low velocities and the higher velocities of the lower crust to the northwest. This abrupt contrast was introduced based on its presence at the northwestern edge of Dalrymple Tough on line 5 (Edwards *et al.* 2008); its presence is consistent with the line 7 data although not constrained by these data. However, a change in crustal velocity structure is clearly evidenced by data from shots to the northwest recorded on OBH 49 (Fig. 2d), which show wide-angle reflections from a mid-crustal discontinuity that does not appear to be present beneath the Trough and higher crustal velocities than those found beneath the Trough (Fig. 2).

Comparison with coincident reflection profile

A depth focusing velocity analysis was conducted independently for the coincident seismic reflection profile SO122–04 (Gaedicke

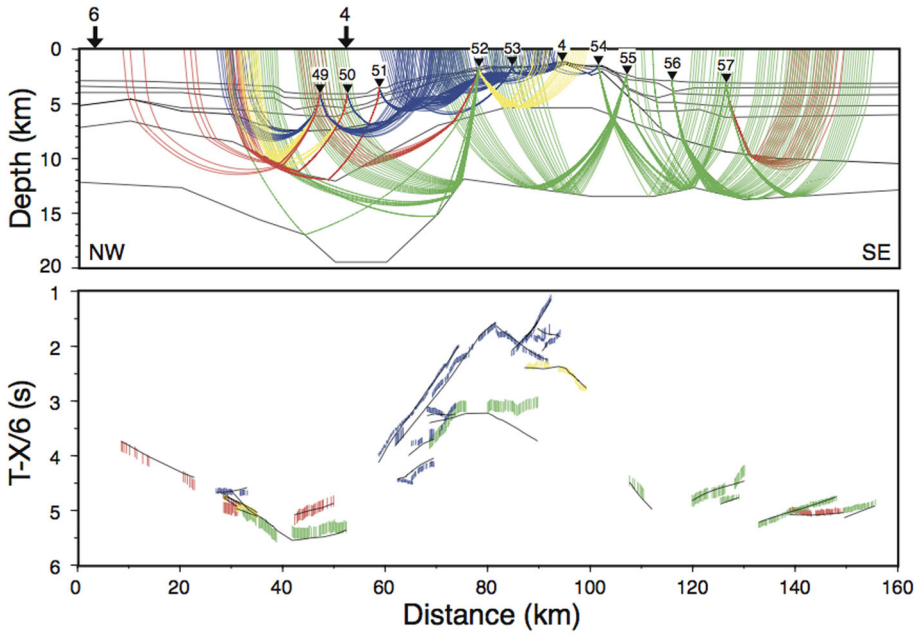

Figure 5. (a) Ray coverage for crustal layers. Rays are plotted for every 3rd traveltime pick. Thin black lines show model boundaries, inverted triangles mark OBH/OBS locations, and arrows mark locations of crossing lines 4 and 6. Blue rays turn in the upper crustal layer and red rays turn in the lower crustal layer, which is the only layer to the southeast of Murray Ridge. Green rays are Moho reflections and yellow rays reflect from a mid-crustal boundary beneath Murray Ridge. (b) Corresponding traveltime fit. Coloured vertical bars show traveltime picks with their uncertainties, with the same colour coding as in (a); black lines show predicted traveltimes.

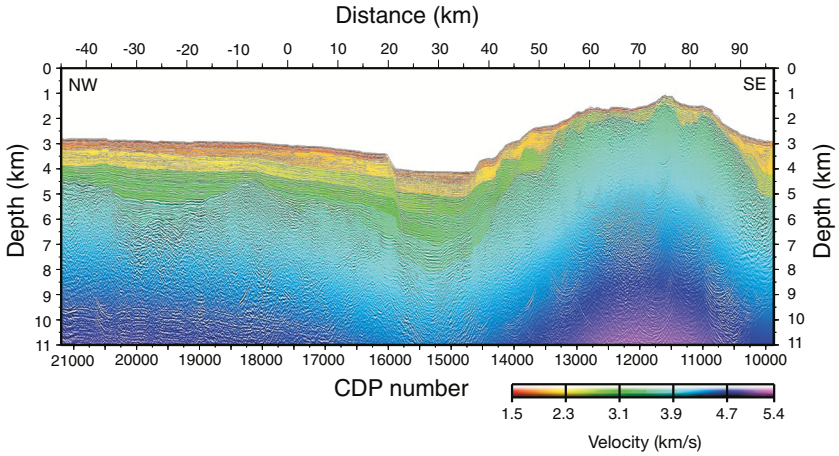

Figure 7. Pre-stack depth migrated image of profile SO122–4 (Gaedicke *et al.* 2002b), with migration velocities overlain.

et al. 2002a; Fig. 6). This analysis yielded very similar velocities for the upper part of the sediment cover. Velocities at depths greater than 2–3 km below the seabed are generally lower than for the velocity model developed above, but at these depths the velocities are poorly constrained by the depth focusing analysis. The depth migrated image (Fig. 7) shows acoustic basement of the Arabian Plate deepening to the southeast from 4.5 km at its shallowest point northwest to 7 km at the northwestern edge of Dalrymple Trough, consistent with the top of the crust in the wide-angle velocity model. If present as a normal incidence reflection, the Moho in this region is obscured by multiples.

Within Dalrymple Trough, layered subhorizontal reflectors appear to extend to 8–9 km depth, though some of these could be pegleg multiples. This is significantly deeper than the top of the crust in the wide-angle velocity model. The difference is not surprising given the complexity of arrivals observed in this region (Fig. 2) and the limited velocity contrast at this boundary. We note also that the depth to the top of the crustal layer in the crossing line 4 is ~10 km in the model of Edwards *et al.* (2008). The apparent thickening of the upper crustal layer into the trough therefore is poorly constrained, and the upper part of the 'crustal' layer in the line 7 model probably comprises old, highly compacted sediments and/or debris from the flanks of the trough. A low-velocity body on the southeast flank of Murray Ridge is inferred from the migration velocity analysis and also appears in the wide-angle seismic model, where it is consistent with rather than required by the data. This body may represent the product of mass wasting from Murray Ridge, as inferred nearby by Edwards *et al.* (2000) and Calves *et al.* (2011).

Interpretation of crustal velocities

Based on the velocity model, the crust on this profile may be divided into three regions: the abyssal plain to the southeast, where it is overlain by thick Indus Fan sediments; the Murray Ridge and Dalrymple Trough regions; and the Gulf of Oman abyssal plain to the northwest. The velocities in the latter region are typical of oceanic crust (Fig. 8a), consistent with other wide-angle seismic studies of the Gulf of Oman (White & Louden 1983; Kopp *et al.* 2000). However, velocities appear to be a little lower than those of oceanic crust at the same depth, and the crustal thickness of up to ~9.5 km is unusually high for oceanic crust. As suggested above for Dalrymple Trough, the crustal layer here may include some sedimentary material at the top; if the upper 1.5 km of the crustal layer is removed, the structure appears to be more consistent with that of normal oceanic crust (Fig. 8a).

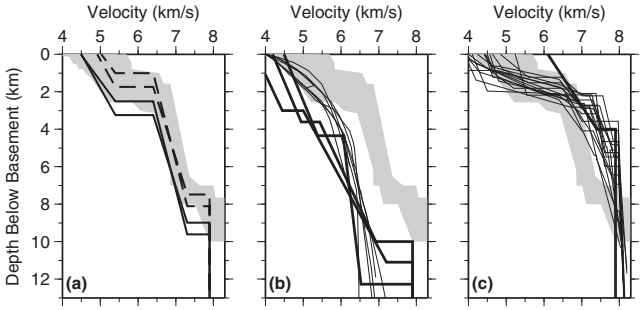

Figure 8. Seismic velocity variation with depth in different parts of the model. In each panel, the grey region marks velocities for 59–170 Ma Atlantic oceanic crust (White *et al.* 1992). (a) Thick solid lines mark seismic velocities at 30 and 40 km model distance (Gulf of Oman abyssal plain). Thick dashed lines mark the same data moved 1.5 km shallower. (b) Thick solid lines mark velocities at 52, 80 and 100 km model distance (Murray Ridge); thin lines mark velocities for island arc crust (Paulatto *et al.* 2010), aligned such that the velocity at the top of basement is 4.0 km s^{-1}. (c) Thick solid lines mark velocities at 116 and 126 km model distance (Indus Fan); thin lines mark velocities for exhumed mantle in the southern Iberia Abyssal Plain (Chian *et al.* 1999; Dean *et al.* 2000).

Crustal velocities beneath Murray Ridge and Dalrymple Trough are much lower than those of oceanic crust and match closely those of modern volcanic arcs (Fig. 8b). The presence of arc crust would be consistent with the recovery of mafic and ultramafic rocks with an inferred supra-subduction zone origin from the crest of Murray Ridge (Burgath *et al.* 2002). It would also be consistent with inferred widespread Neoproterozoic arc volcanism on the western margin of the Indian craton (Torsvik *et al.* 2013), although Burgath *et al.* (2002) suggest a younger, Cretaceous age for these rocks.

To the southeast, crustal velocities are significantly higher and resemble neither those of oceanic crust nor those of Murray Ridge and Dalrymple Trough, and the crust is only 4 km thick. These velocities are consistent with the presence of mafic lower continental crust exhumed by high degrees of extension. They also resemble those of exhumed serpentinized mantle in the southern Iberia Abyssal Plain (Chian *et al.* 1999; Dean *et al.* 2000; Fig. 8c). Velocities less than 6 km s^{-1}, that are normally present when the mantle is exhumed, are absent here, but a thin (<1–2 km) layer of velocities in the

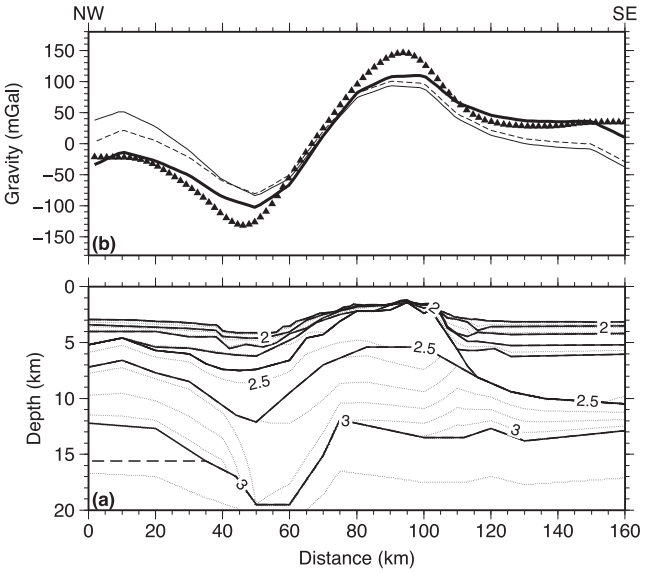

Figure 9. (a) Density model derived from the velocity model in Fig. 6. Contours are labelled in Mg m^{-3} and contour interval is 0.1 Mg m^{-3}. Thick dashed line shows alternative model with deeper Moho in the northwest. (b) Triangles show satellite-derived gravity from global grid (Sandwell & Smith 1997). Thin solid line marks calculated gravity anomaly of the model shown in (a), with horizontal density contours extending far enough from the model edges to remove edge effects. Dashed line marks calculated anomaly for the model with the deeper Moho in (a). Thick solid line marks calculated anomaly for a model with a horizontal density gradient in the mantle that is sufficient to reproduce the observed gravity difference between the two ends of the profile.

range 5–6 km s^{-1} would not yield first arrivals and could easily be obscured by the thick sedimentary cover. Whichever interpretation is valid, the wide-angle seismic data are consistent with the presence of highly extended continental lithosphere, and not with the presence of oceanic crust.

Constraints from gravity data

Gravity data provide an important independent constraint on crustal structure. To take advantage of this constraint, we converted our velocity model to a density model using a fourth-order polynomial fit to the regression of Ludwig *et al.* (1970). The density of sea water was fixed at 1.03 kg m^{-3}. We then computed the gravity anomaly using the method of Talwani *et al.* (1959), and compared the resulting anomaly with the satellite-derived gravity anomaly of Sandwell & Smith (1997). This calculation yielded a generally good fit at short wavelengths, but a large long-wavelength misfit (Fig. 9). The good short-wavelength fit provides support for our interpretation of the deep reflecting boundary in the velocity model as the Moho, and for its modelled shape. The reduced amplitude of the calculated gravity anomaly compared with the observed anomaly may be attributed to deviations from a 2-D structure: the bathymetric features associated with Murray Ridge and Dalrymple Trough are not parallel to each other and our profile is not perpendicular to either (Fig. 1).

We explored whether the long-wavelength misfit could be explained by using a different crustal thickness in the poorly constrained northwestern part of the profile, but increasing the crustal thickness by up to 50 per cent yields little improvement on the long-wavelength fit (Fig. 9). A long-wavelength gravity anomaly should be generated in the region by the bending of the oceanic lithosphere into the Makran subduction zone. However, the northwestern end of our profile is over 100 km from the deformation front of the subduction zone and oblique to the dip of the slab, and slab dip beneath the subduction zone is very gentle (e.g. Kopp *et al.* 2000), so we do not anticipate a significant gravity anomaly along our profile due to the slab.

Therefore, we attribute the long-wavelength misfit to along-profile density variations in the mantle lithosphere. The misfit can be removed by a linear variation in density along the profile of mantle material shallower than 25 km depth (Fig. 9). The 25 km depth limit is an arbitrary choice for computational convenience, and mantle density variations are likely to be spread over a much greater depth interval, but the calculations illustrate that a denser or thicker, and hence thermally older, lithosphere is required to the southeast. A more realistic approach would be to attribute the long-wavelength misfit to temperature differences arising from differences in age across the plate boundary (e.g. Leitner *et al.* 1998). Because of the lack of identifiable magnetic anomaly lineations, the age of the lithosphere is poorly known on both sides of the plate boundary. Therefore we carried out a simple calculation of the gravity difference between oceanic lithospheric thermal structures for a wide range of different ages, using the infinite slab approximation, to determine what magnitude of age difference might be required to explain the gravity change across the plate boundary.

We used two different plate cooling models: the model of Parsons & Sclater (1977) and the GDH1 model of Stein & Stein (1992). We have established above that the lithosphere beneath the Indus Fan does not have an oceanic structure, so strictly our calculation is not valid for this region. However, in a pure shear model the thermal structure of highly stretched continental lithosphere approximates closely that of oceanic lithosphere of the same age as the extension event, as does that of exhumed mantle if the switch to simple shear extension occurs during the late stages of continental breakup (e.g. Whitmarsh *et al.* 2001). The slab approximation is strictly only valid far from the plate boundary, but without detailed knowledge of the history of the plate boundary a more sophisticated approach is not possible.

For both thermal models, a large age difference is required (Fig. 10), which is consistent also with the large difference in basement depth between the two ends of our model. Based on plate reconstructions, the oceanic lithosphere in the Gulf of Oman is interpreted to be either Jurassic to early Cretaceous or Palaeocene to Eocene in age (Mountain & Prell 1990). The long-wavelength gravity anomaly could not be explained by a Jurassic to early Cretaceous age because in this scenario, the associated gravity anomaly would be too small (Fig. 10). A Palaeocene to Eocene age gives a large anomaly if the lithosphere to the southeast is Jurassic in age, though even then the predicted gravity difference is only just sufficient. Since many approximations are involved in this analysis, it should be seen as illustrative only, but we infer that the oceanic crust in the Gulf of Oman adjacent to Dalrymple Trough is Palaeogene in age, as inferred by Edwards *et al.* (2000) and that the adjacent lithosphere beneath the Indus Fan is much older.

Nature and origin of the lithosphere in the Northeast Arabian Sea

Our results place some new constraints on the nature and origin of the poorly known region of lithosphere between the Indian continent and the first clearly identified seafloor spreading anomalies generated by the Carlsberg Ridge (Fig. 11). Based on wide-angle seismic

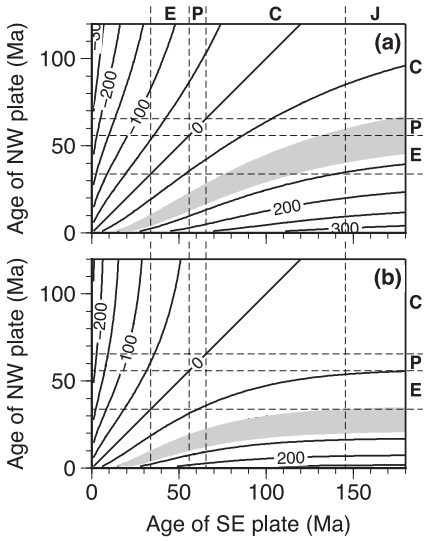

Figure 10. Gravity difference between two cooling lithospheric plates, in the infinite slab approximation, as a function of age difference between them. Grey region marks the gravity difference between the two ends of the profile in Fig. 9 that cannot be explained by the crustal structure, estimated at 90–135 mGal. Bar at the top marks the periods mentioned in the text, with J marking Jurassic, C Cretaceous, P Paleaocene and E Eocene. (a) Plate cooling model of Parsons & Sclater (1977). (b) Cooling model of Stein & Stein (1992).

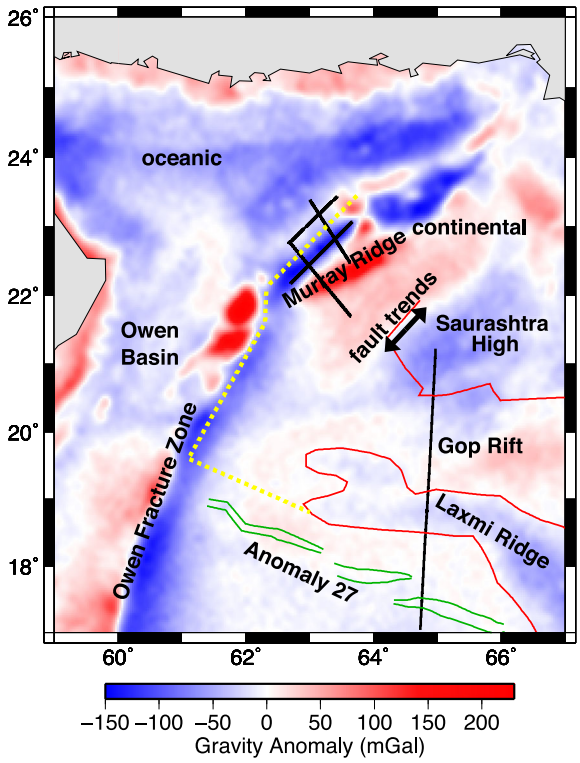

Figure 11. Free-air gravity of the northwest Indian Ocean with main tectonic features. Thick black lines are wide-angle seismic profiles (this paper and Minshull *et al.* 2008). Green lines are magnetic anomaly picks (Miles *et al.* 1998), and red lines outline the gravity low associated with Laxmi Ridge and the basement high identified by Malod *et al.* (1997) and subsequently named the Saurashtra High. Arrows mark basement fault trend identified by Malod *et al.* (1997). Dashed yellow line marks our proposed ocean–continent boundary. Oceanic crust is also likely to be present in the Gop Rift (e.g. Bhattacharya *et al.* 1994; Minshull *et al.* 2008), but in our interpretation this crust must taper out near the western tip of Laxmi Ridge.

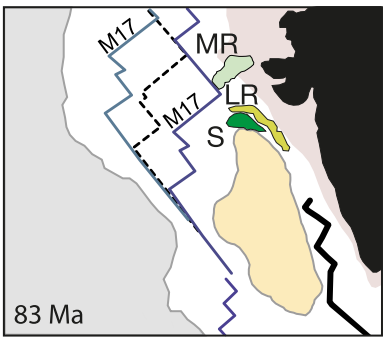

Figure 12. Plate reconstruction at 83 Ma, simplified from Calves *et al.* (2011). In this reconstruction, India is fixed and Murray Ridge (MR) is fixed with India, while Gop Rift and the Mascarene Basin are closed. Blue lines are magnetic anomalies, LR is Laxmi Ridge and S (dark green) is the Seychelles platform.

constraints (Minshull *et al.* 2008) and the nature of acoustic basement (Malod *et al.* 1997), a region of shallow basement and negative free air gravity anomaly *ca*. 100 km to the southeast of our profile has been identified as stretched continental crust. More recently, extensive industry seismic reflection data have shown the widespread presence of volcanics in this region, which has been subsequently named the Saurashtra High or Saurashtra Volcanic Platform. These data have led to an interpretation as highly stretched (10–12 km) continental crust overlain by thick volcanics or even as an oceanic plateau (Corfield *et al.* 2010; Calves *et al.* 2011). To the southwest of this basement high, in the Gop Rift and its northwestern extension, the presence of oceanic crust is inferred from wide-angle seismic data (Minshull *et al.* 2008), from seismic reflection profiles exhibiting a typical oceanic Moho (Calves *et al.* 2011) and from the presence of linear magnetic anomalies. The sequence of anomalies is too short to allow their age to be determined uniquely, and their age remains controversial (Collier *et al.* 2008; Yatheesh *et al.* 2009; Armitage *et al.* 2011), but they are generally attributed a Late Cretaceous age.

Calves *et al.* (2011) interpret the crust between the Saurashtra High and Murray Ridge as oceanic crust formed by the same broadly north–south spreading system as the Gop Rift. However, northeast–southwest striking basement fabrics are identified in this region by Malod *et al.* (1997) and a northeast–southwest volcanic basement ridge, the Somnath Ridge, is present immediately to the northwest of the Saurashtra High (Calves *et al.* 2011). Both features are consistent with northwest–southeast extension in this region, though the abrupt northwestern edge of the Saurathtra High has alternatively been interpreted as evidence for a transform margin here (Corfield *et al.* 2010; Calves *et al.* 2011). We therefore infer that extension in this region predates the formation of the Gop Rift and, based on our seismic velocity constraints, propose an ocean–continent transition further to the southwest than that proposed by Calves *et al.* (2011; Fig. 11).

Finally, we explore the possible tectonic setting of this inferred earlier extension episode that separated the Murray Ridge from the Saurashtra High. To do this we must close both the northwest Indian Ocean and the Gop Rift, since we have inferred that these features postdate this extension. Prior to the opening of the Gop Rift, the southeastern margin of the Murray Ridge, and therefore the strike of the inferred extension direction, is parallel to seafloor-spreading isochrons in the West Somali Basin (Fig. 12). Note that although

we have used the reconstruction of Calves *et al.* (2011), we obtain the same orientation (though different location) for this boundary with a range of other reconstructions. We therefore speculate that this small, 100-km-wide basin is a failed rift that formed between Somalia and Madagascar during the *ca*. 153 Ma opening of the Somali Basin (Rabinowicz *et al.* 1983). Based on seismic reflection and gravity data, Corfield *et al.* (2010) infer a similar age for this basin, though they prefer an oceanic origin and implicitly a different direction of extension. This extensional episode may also explain thick pre-Deccan sedimentary deposits onshore in the Katchchh peninsula (e.g. Pandey *et al.* 2009).

CONCLUSIONS

From our wide-angle seismic study of the Murray Ridge and adjacent regions, we conclude that:

(1) The Murray Ridge is a continental fragment possibly formed originally by Neoproterozoic arc volcanism and separated from India during the opening of the West Somali Basin.

(2) A long-wavelength mantle density contrast is required between the lithosphere of the western continental margin of India, to the southwest of Murray Ridge, and the lithosphere of the Arabian Sea. This density contrast may be attributed to a large age contrast across the plate boundary in Dalrymple Trough.

(3) The basement beneath the adjacent Indus Fan sediments is composed either of highly thinned continental crust or of exhumed serpentinized mantle.

ACKNOWLEDGEMENTS

We thank captain H. Andresen and the officers and crew of the RV Sonne during cruise SO-123, and all colleagues who participated on the cruise. The cruise was funded by the German Federal Ministry for Science and Technology (BMBF grant 03G0123A) and by the EU through the programme Access to Large Scale Facilities. The depth migration of Fig. 7 was carried out by Christian Kopp at Geomar. We thank Gail Christeson and Anne Trehu for careful reviews.

REFERENCES

Armitage, J.J., Collier, J.S., Minshull, T.A. & Henstock, T.J., 2011. Thin oceanic crust and flood basalts: India-Seychelles breakup, *Geochem. Geophys. Geosyst.,* **12,** Q0AB07, doi:10.1029/2010GC003316.

ArRajehi, A. *et al.*, 2010. Geodetic constraints on present-day motion of the Arabian Plate: implications for Red Sea and Gulf of Aden rifting, *Tectonics,* **29,** TC3011, doi:10.1029/2009tc002482.

Bhattacharya, G.C., Chaubey, A.K., Murty, G.P.S., Srinivas, K., Srama, K.V.L.N.S., Subrahmanyam, V. & Krishna, K.S., 1994. Evidence for seafloor spreading in the Laxmi Basin, northeastern Arabian Sea, *Earth planet. Sci. Lett.,* **125,** 211–220.

Burgath, K.P., Von Rad, U., Van Der Linden, W., Block, M., Khan, A.A., Roeser, H.A. & Weiss, W., 2002. Basalt and peridotite recovered from Murray Ridge: are they of supra-subduction origin?, in *Tectonic and Climatic Evolution of the Arabian Sea Region,* pp. 117–135, eds Clift, P.D., Kroon, D., Gaedicke, C. & Craig, J., Geological Soc. Publishing House.

Calves, G., Schwab, A.M., Huuse, M., Clift, P.D., Gaina, C., Jolley, D., Tabrez, A.R. & Inam, A., 2011. Seismic volcanostratigraphy of the western Indian rifted margin: the pre-Deccan igneous province, *J. geophys. Res.: Solid Earth,* **116,** B01101, doi:10.1029/2010jb000862.

Chian, D., Louden, K.E., Minshull, T.A. & Whitmarsh, R.B., 1999. Deep structure of the ocean-continent transition in the southern Iberia Abyssal Plain from seismic refraction profiles: ocean Drilling Program (Legs 149 and 173) transect, *J. geophys. Res.,* **104,** 7443–7462.

Collier, J.S., Sansom, V., Ishizuka, O., Taylor, R.N., Minshull, T.A. & Whitmarsh, R.B., 2008. Age of Seychelles-India break-up, *Earth planet. Sci. Lett.,* **272,** 264–277.

Corfield, R.I., Carmichael, S., Bennett, J., Akhter, S., Fatimi, M. & Craig, T., 2010. Variability in the crustal structure of the West Indian Continental Margin in the Northern Arabian Sea, *Petrol. Geosci.,* **16,** 257–265.

Dean, S.M., Minshull, T.A., Whitmarsh, R.B. & Louden, K., 2000. Deep structure of the ocean-continent transition in the southern Iberia Abyssal Plain from seismic refraction profiles: II. The IAM-9 transect at 40°20′N, *J. geophys. Res.,* **105,** 5859–5886.

Demets, C., Gordon, R.G., Argus, D.F. & Stein, S., 1990. Current plate motions, *Geophys. J. Int.,* **101,** 425–478.

Edwards, R.A., Minshull, T.A. & White, R.S., 2000. Extension across the Indian-Arabian plate boundary: the Murray Ridge, *Geophys. J. Int.,* **142,** 461–477.

Edwards, R.A., Minshull, T.A., Flueh, E.R. & Kopp, C., 2008. Dalrymple Trough: an active oblique-slip ocean-continent boundary in the northwest Indian Ocean, *Earth planet. Sci. Lett.,* **272,** 437–445.

Fournier, M., Chamotrooke, N., Petit, C., Fabbri, O., Huchon, P., Maillot, B. & Lepvrier, C., 2008. In situ evidence for dextral active motion at the Arabia-India plate boundary, *Nat. Geosci.,* **1,** 54–58.

Fournier, M., Chamot-Rooke, N., Rodriguez, M., Huchon, P., Petit, C., Beslier, M.O. & Zaragosi, S., 2011. Owen fracture zone: the Arabia-India plate boundary unveiled, *Earth planet. Sci. Lett.,* **302,** 247–252.

Gaedicke, C., Prexl, A., Schluter, H.U., Meyer, H., Roeser, H. & Clift, P., 2002a. Seismic stratigraphy and correlation-of major regional unconformities in the northern Arabian Sea, in *Tectonic and Climatic Evolution of the Arabian Sea Region,* pp. 25–36, eds Clift, P.D., Kroon, D., Gaedicke, C. & Craig, J. Geological Soc. Publishing House.

Gaedicke, C. *et al.*, 2002b. Origin of the northern Indus Fan and Murray Ridge, Northern Arabian Sea: interpretation from seismic and magnetic imaging, *Tectonophysics,* **355,** 127–143.

Gordon, R.G. & Demets, C., 1989. Present-day motion along the Owen Fracture Zone and Dalrymple Trough in the Arabian Sea, *J. geophys. Res.: Solid Earth Planets,* **94,** 5560–5570.

Kopp, C., Fruehn, J., Flueh, E.R., Reichert, C., Kukowski, N., Bialas, J. & Klaeschen, D., 2000. Structure of the Makran subduction zone from wide-angle and reflection seismic data, *Tectonophysics,* **329,** 171–191.

Korenaga, J., Holbrook, W.S., Kent, G.M., Kelemen, P.B., Detrick, R.S., Larsen, H.-C., Hopper, J.R. & Dahl-Jensen, T., 2000. Crustal structure of the southeast Greenland margin from joint refraction and reflection seismic tomography, *J. geophys. Res.,* **105,** 21 591–21 614.

Leitner, B., Trehu, A.M. & Godfrey, N.J., 1998. Crustal structure of the northwestern Vizcaino block and Gorda Escarpment, offshore northern California, and implications for postsubduction deformation of a paleoaccretionary margin, *J. geophys Res.: Solid Earth,* **103,** 23 795–23 812.

Ludwig, W.J., Nafe, J.E. & Drake, C.L., 1970. Seismic refraction, in *The Sea,* pp. 53–84, ed. Maxwell, A.E., Wiley Interscience.

Malod, J., Droz, L., Mustafa Kemal, B. & Patriat, P., 1997. Early spreading and continental to oceanic basement transition beneath the Indus deep-sea fan: N.E. Arabian Sea, *Mar. Geol.,* **141,** 221–235.

Miles, P.R., Munschy, M. & Segoufin, J., 1998. Structure and early evolution of the Arabian Sea and East Somali Basin, *Geophys. J. Int.,* **134,** 876–888.

Minshull, T.A., Lane, C.I., Collier, J.S. & Whitmarsh, R.B., 2008. The relationship between rifting and magmatism in the northeastern Arabian Sea, *Nat. Geosci.,* **1,** 463–467.

Mountain, G.S. & Prell, W.L., 1990. A multiphase plate tectonic history of the southeast continental margin of Oman, in *The Geology and Tectonics of the Oman Region,* pp. 725–743, eds Robertson, A.H.F., Searle, M.P. & Ries, A.C. Geological Soc. Publishing House.

Pandey, D., Singh, S., Sinha, M. & MacGregor, L., 2009. Structural imaging of Mesozoic sediments of Kachchh, India, and their hydrocarbon prospects, *Mar. Pet. Geol.,* **26,** 1043–1050.

Parsons, B. & Sclater, J.G., 1977. Analysis of variation of ocean-floor bathymetry and heat-flow with plate age, *J. geophys. Res.,* **82,** 803–827.

Paulatto, M. *et al.*, 2010. Upper crustal structure of an active volcano from refraction/reflection tomography, Montserrat, Lesser Antilles, *Geophys. J. Int.,* **180,** 685–696.

Quittmeyer, R.C. & Kafka, A.L., 1984. Constraints on plate motions in southern Pakistan and the northern Arabian Sea from the focal mechanisms of small earthquakes, *J. geophys. Res.,* **89,** 2444–2458.

Rabinowicz, P.D., Coffin, M.F. & Falvey, D., 1983. The separation of Madagascar and Africa, *Science,* **220,** 67–69.

Sandwell, D.T. & Smith, W.H.F., 1997. Marine gravity anomaly from Geosat and ERS 1 satellite altimetry, *J. geophys Res.: Solid Earth,* **102,** 10 039–10 054.

Stein, C.A. & Stein, S., 1992. A model for the global variation in oceanic depth and heat-flow with lithospheric age, *Nature,* **359,** 123–129.

Talwani, M., Worzel, J.L. & Landisman, M., 1959. Rapid gravity computations for two-dimensional bodies with application to the Mendocino submarine fracture zone, *J. geophys. Res.,* **64,** 49–59.

Torsvik, T.H. *et al.*, 2013. A Precambrian microcontinent in the Indian Ocean, *Nat. Geosci.,* **6,** 223–227.

White, R.S. & Louden, K.E., 1983. The Makran continental margin: structure of a thickly sedimented convergent plate boundary, in *Studies in Continental Margin Geology,* pp. 499–518, eds Watkins, J.S. & Drake, C.L., American Association of Petroleum Geologists.

White, R.S., McKenzie, D. & O'Nions, K., 1992. Oceanic crustal thickness from seismic measurements and rare earth element inversions, *J. geophys. Res.,* **97,** 19 683–19 715.

Whitmarsh, R.B., Manatschal, G. & Minshull, T.A., 2001. Evolution of magma-poor continental margins from final rifting to seafloor spreading, *Nature,* **413,** 150–154.

Yatheesh, V., Bhattacharya, G.C. & Dyment, J., 2009. Early oceanic opening off Western India-Pakistan margin: the Gop Basin revisited, *Earth planet. Sci. Lett.,* **284,** 399–408.

Zelt, C.A. & Barton, P.J., 1998. Three-dimensional seismic refraction tomography: a comparison of two methods applied to date from the Faeroe Basin, *J. geophys. Res.,* **103,** 7187–7210.

Zelt, C.A. & Smith, R.B., 1992. Seismic traveltime inversion for 2-D crustal velocity structure, *Geophys. J. Int.,* **108,** 16–34.